

In-phase evanescent coupling of two-dimensional arrays of defect cavities in photonic crystal vertical cavity surface emitting lasers

James J. Raftery, Jr.,^{a)} Ann C. Lehman, Aaron J. Danner,^{b)} Paul O. Leisher, Antonios V. Giannopoulos, and Kent D. Choquette
Micro and Nanotechnology Laboratory, Department of Electrical and Computer Engineering, University of Illinois, 208 N. Wright St., Urbana, Illinois 61801

(Received 13 February 2006; accepted 27 June 2006; published online 24 August 2006)

In-phase evanescent coupling in 2×1 and 2×2 arrays of defect cavities in photonic crystal (PhC) vertical cavity surface emitting lasers (VCSELs) is reported. Two-dimensional PhC patterns of air holes containing multiple defects are etched into the top distributed Bragg reflector of VCSELs. The resulting modification of the effective index and optical loss results in evanescent coupling between the multiple defect cavities of the PhC VCSEL. Far field measurements and simulations show good agreement and demonstrate the in-phase results. © 2006 American Institute of Physics.

[DOI: 10.1063/1.2336618]

Coherently coupled two-dimensional (2D) arrays of vertically emitting lasers offer the potential of extended area coherent sources with high spectral purity, useful in a variety of applications in the high power (laser radar, optical communications, steerable sources) and low power (image processing, spectroscopic sensing, optical logic) regimes. Evanescent coupling between array elements of vertical cavity surface emitting lasers (VCSELs) has been studied extensively.¹⁻⁵ A major disadvantage of this approach is that the large inherent optical loss between neighboring cavities results in out-of-phase operation for those coherently coupled devices.⁶ For the applications listed earlier, in-phase coherently coupled operation is generally preferred. In-phase coherent coupling is achieved when the phase difference of the electric fields between neighboring cavities is zero, and is manifested in the far field by a central on-axis lobe with subsidiary side lobes. Such a far field has been achieved using a phase-adjusted array⁷ and antiguided VCSEL arrays to achieve the in-phase coupling.^{8,9} We report an approach for modification of the effective index and optical loss in the coupling regions between the defect cavities for achieving evanescent in-phase coherently coupled operation.

A photonic crystal (PhC) VCSEL is created when a 2D PhC lattice of air holes is etched into the top distributed Bragg reflector (DBR) of a VCSEL thereby defining a lasing cavity confined within a defect of the PhC lattice.^{10,11} When multiple defects are introduced, evanescent transverse coupling between the defect cavities can result. It has previously been reported that PhC VCSELs with multiple defect cavities operate out-of-phase coherently coupled for both a 2×1 array¹² and a 2×2 array¹³ of defect cavities. Here we report in-phase coherent coupling for both 2×1 and 2×2 arrays of defect cavities in PhC VCSELs.

In order to obtain these results, selectively oxidized 850 nm VCSELs, created with a mesa etch process¹⁴ were first fabricated and characterized. To create the PhC VCSELs, a layer of SiO₂ was deposited over the top facet of the lasers. The 2D triangular lattice hole patterns were then

etched through the SiO₂ using electron beam lithography followed by a Freon reactive ion etch, with the multiple defect cavities designed into the photonic crystal lattice by omitting selected holes. The patterns were then etched down into the top DBR of each VCSEL by an inductively coupled plasma reactive ion etch utilizing silicon tetrachloride, thereby creating the air holes. This is a relatively straightforward and robust fabrication process for achieving coherent coupling in vertically emitting lasers.¹⁵

Figure 1(a) shows a PhC design with a 2×1 array of defects that resulted in evanescent in-phase coherent coupling. The PhC lattice constant, a , is $4.0 \mu\text{m}$ and the hole-diameter-to-lattice-constant ratio, b/a , is 0.70. The air hole located in the coupling region between the two defects has a reduced hole-diameter-to-lattice-constant ratio, b'/a , of 0.55. This device is from a series of ten devices where this coupling region b'/a parameter was varied from 0.25 to 0.70 in steps of 0.05. These devices were fabricated into VCSEL material with a n -type top DBR containing 25 mirror periods. The holes in the PhC pattern were etched down approximately 19 periods, while the coupling region hole for this device was etched approximately two periods less due to plasma loading effects. Varying the hole diameter and depth in the coupling region modifies both the refractive index and optical loss in the coupling region and has been shown to effect cavity coupling.¹³ Figure 1(b) shows the near field

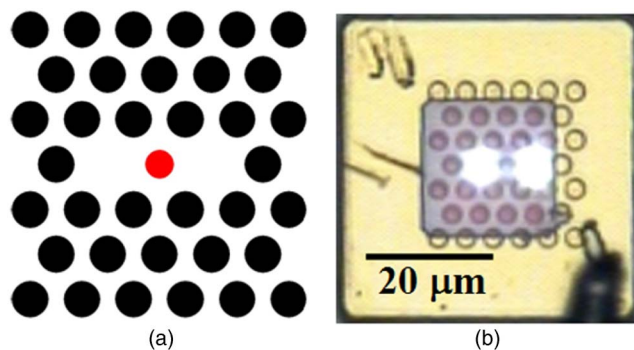


FIG. 1. (Color online) (a) PhC pattern with a 2×1 array of defect cavities. The hole located in the coupling region has a hole diameter of $2.2 \mu\text{m}$. (b) Near field image of the fabricated PhC VCSEL operating in-phase coherently coupled at an injection current of approximately twice threshold.

^{a)}Present address: Photonics Research Center at the U.S. Military Academy, West Point, NY; electronic mail: jim.raftery@usma.army.mil

^{b)}Present address: Avago Technologies, Singapore.

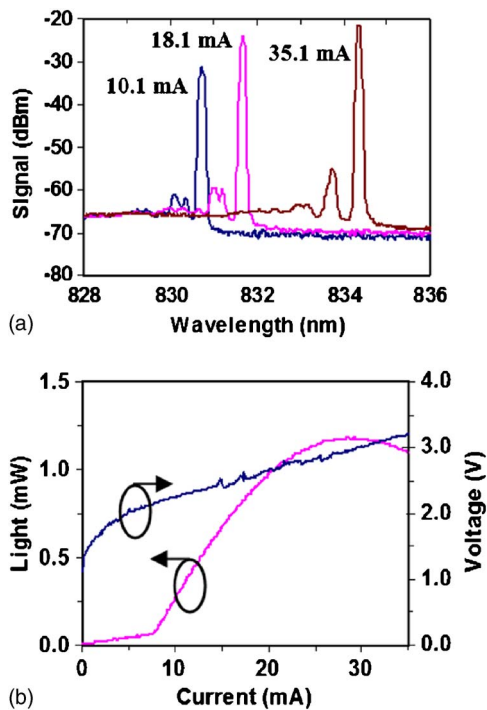


FIG. 2. (Color online) (a) Spectral data and (b) light output and applied voltage data for the device of Fig. 1(b), respectively.

image of the device with two PhC defect cavities operating at room temperature continuous wave cw at an injection current of 18.1 mA. The spectral data are shown in Fig. 2(a), while the optical power and voltage versus injection current plots are shown in Fig. 2(b). Single mode operation (>30 dB) is observed from threshold to beyond the maximum power condition.

Figure 3 illustrates the in-phase coherent coupling, measured at an injection current of 18.1 mA. Figure 3(a) is the measured far field intensity contour plot and Fig. 3(b) provides the same data as a height coded intensity plot. A central on-axis lobe is observed with two subsidiary side lobes. Dis-

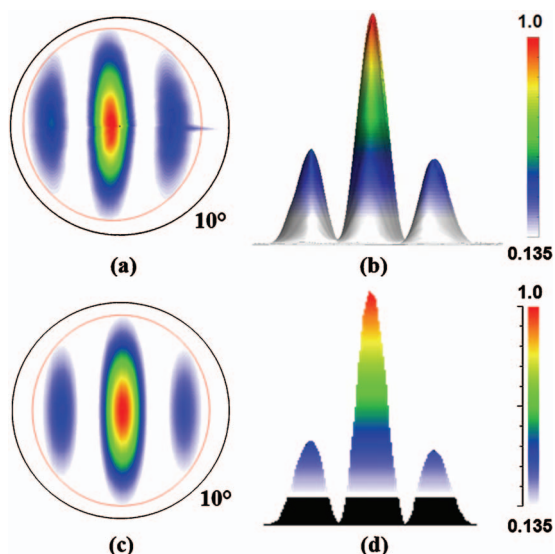


FIG. 3. (Color) (a) Measured far field intensity contour plot and (b) height coded intensity plot for the device of Fig. 1(b) showing in-phase operation. (c) Calculated far field intensity contour plot and (d) height coded intensity plot. In (a) and (c) a circle showing the 10° angular width from the optical axis is provided, while the inner ellipse is fitted to the plot.

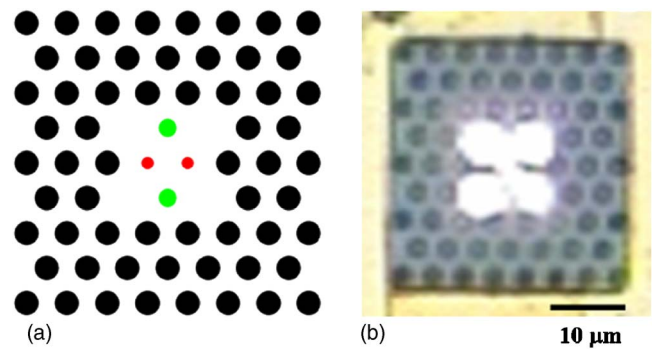


FIG. 4. (Color online) (a) PhC pattern with a 2×2 array of defect cavities. The top and bottom coupling region hole diameters are $1.8 \mu\text{m}$, and the left and right coupling region hole diameters are $1.2 \mu\text{m}$. (b) Near field image of the fabricated PhC VCSEL operating in-phase coherently coupled at an injection current of approximately 1.2 times threshold.

tinct nulls are observed between the lobes, indicative of a high degree of coherence between the two cavities and relatively equal lasing intensity in the two cavities.¹⁶ Analysis of the far field pattern of Fig. 3(b) indicates that an approximately 10° relative phase difference between the emitted beams occurs at this injection current.¹⁷ Figure 3(a) shows an ellipse fitted to the measured data, which by application of the diffraction limit to the Gaussian-like emitted beams, gives the near field mode size ($1/e^2$ intensity) as elliptical with major and minor axes of approximately 3.8 and $3.5 \mu\text{m}$, respectively. These factors were included into a beam propagation method simulation,¹³ and the calculated results are shown as Figs. 3(c) and 3(d), respectively, showing the measured and calculated far field plots to be in good agreement.

Of the ten 2×1 defect cavity devices in this series of arrays with varying center hole, three showed far fields indicative of in-phase coupling (b'/a of 0.45, 0.55, and 0.60). Using a larger center hole produced uncoupled arrays (b'/a of 0.65 and 0.70), while smaller central holes generally produced out-of-phase coherent coupling (b'/a of 0.25, 0.30, 0.35, 0.40, and 0.50). The mechanisms for achieving in-phase coupling are attributed to the unique method of defining the lasing cavity by the PhC in the DBR mirror, along with the variation of the air hole parameters in the coupling region between defect cavities. Since the defects share a common gain region, and the transverse confinement induced by the PhC is located in the DBR where the longitudinal field is reduced, the inherent optical loss in the coupling region is also reduced as compared to evanescently coupled arrays with pixelated gain regions.¹⁻⁷ Instead of the lowest order (in-phase) mode being discriminated against due to higher optical loss, this mode is now observed in PhC VCSEL arrays.

Figure 4(a) shows a PhC design with a 2×2 array of defects that also produce in-phase coherent coupling. The PhC lattice constant is $4.0 \mu\text{m}$ and the hole-diameter-to-lattice-constant ratio is 0.6. As shown in Fig. 4(a) the two coupling region air holes located at the top and bottom of the coupling region have a reduced hole-diameter-to-lattice-constant ratio of 0.45, while the two coupling regions' holes located at the left and right of the coupling region have a reduced hole-diameter-to-lattice-constant ratio of 0.30. This device was fabricated into VCSEL material with a p -type top DBR containing 19 mirror periods. The holes in the PhC pattern were etched down approximately 15 periods, and the

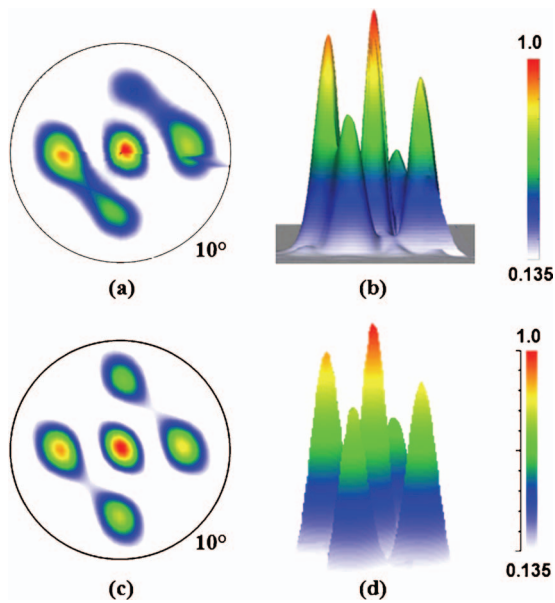


FIG. 5. (Color) (a) Measured far field intensity contour plot and (b) height coded intensity plot for the device of Fig. 4(b) showing in-phase operation. (c) Calculated far field intensity contour plot and (d) height coded intensity plot.

coupling region holes were etched approximately two to three periods less. Figure 4(b) shows the near field image of the device with four PhC defect cavities operating at room temperature cw in-phase coherently coupled at an injection current of 1.2 times threshold. The near field shows an additional optical intensity lobe located in the area at the center between the four coupling region holes. A similar intensity lobe was also observed and exploited in leaky mode VCSEL arrays.⁸ This device exhibited an in-phase coupled far field pattern from threshold to the maximum power condition (1.6 mW). A single dominant spectral peak (not shown) is observed over this operating range.

Figures 5(a) and 5(b) show the measured far field intensity contour plot and height coded intensity plot, respectively. A central on-axis lobe is observed, with four subsidiary side lobes. Intensity differences between the far field lobes are clearly evident. The asymmetries in the spacing between the defect cavities, due to the geometry of the triangular PhC lattice explain why the left and right side lobes have a greater intensity than the top and bottom side lobes.¹³ Simulations were conducted that included intensity differences between defect cavities, a phase difference for one cavity, and a fifth lasing area at the center of the coupling region, which is 180° out-of-phase. Figures 5(c) and 5(d)

show the calculated results for the far field intensity contour plot and the height coded intensity plot, respectively, which follow the measured data. These simulations suggest that varying the four PhC holes between the four defects again produces a reduction of loss such that the lowest order in-phase mode can operate.

In summary, evanescent in-phase coherent coupling in 2×1 and 2×2 arrays of defect cavities in PhC VCSELs is reported. Far field measurements were presented to demonstrate the in-phase results, and agreement between the measured and simulated in-phase far fields is shown. Modification of the effective refractive index and optical loss in the coupling regions between the defect cavities is the proposed mechanism that enables evanescent in-phase coherent coupling. Further investigation of the mode selection and optical coherence in these arrays is ongoing.

This work is supported by the United States Army under Award No. DAAD19-03-1-0299 and by the Defense Advanced Research Projects Agency under Award No. 317271-7830.

- ¹H.-J. Yoo, A. Scherer, J. P. Harbison, L. T. Florenz, E. G. Paek, B. P. Van der Gaag, J. R. Hayes, A. Von Lehmen, E. Kapon, and Y.-S. Kwon, *Appl. Phys. Lett.* **56**, 1198 (1990).
- ²D. G. Deppe, J. P. van der Ziel, N. Chand, G. J. Zyzdik, and S. N. G. Chu, *Appl. Phys. Lett.* **56**, 2089 (1990).
- ³M. Orenstein, E. Kapon, N. G. Stoffel, J. P. Harbison, L. T. Florenz, and J. Wullert, *Appl. Phys. Lett.* **58**, 804 (1991).
- ⁴P. L. Gourley, M. E. Warren, G. R. Hadley, G. A. Vawter, T. M. Brennan, and B. E. Hammons, *Appl. Phys. Lett.* **58**, 890 (1991).
- ⁵S. Riyopoulos, *Phys. Rev. A* **66**, 053820 (2002).
- ⁶G. R. Hadley, *Opt. Lett.* **15**, 1215 (1990).
- ⁷M. E. Warren, P. L. Gourley, G. R. Hadley, G. A. Vawter, T. M. Brennan, B. E. Hammons, and K. L. Lear, *Appl. Phys. Lett.* **61**, 1484 (1992).
- ⁸D. K. Serkland, K. D. Choquette, G. R. Hadley, K. M. Geib, and A. A. Allerman, *Appl. Phys. Lett.* **75**, 3754 (1999).
- ⁹D. Zhou and L. J. Mawst, *Appl. Phys. Lett.* **77**, 2307 (2000).
- ¹⁰D.-S. Song, S.-H. Kim, H.-G. Park, C.-K. Kim, and Y.-H. Lee, *Appl. Phys. Lett.* **80**, 3901 (2002).
- ¹¹N. Yokouchi, A. J. Danner, and K. D. Choquette, *IEEE J. Sel. Top. Quantum Electron.* **9**, 1439 (2003).
- ¹²A. J. Danner, J. C. Lee, J. J. Raftery, Jr., N. Yokouchi, and K. D. Choquette, *Electron. Lett.* **39**, 1323 (2003).
- ¹³J. J. Raftery, Jr., A. J. Danner, J. C. Lee, and K. D. Choquette, *Appl. Phys. Lett.* **86**, 201104 (2005).
- ¹⁴K. D. Choquette, K. L. Lear, R. P. Schneider, Jr., K. M. Geib, J. J. Figiel, and R. Hull, *IEEE Photonics Technol. Lett.* **7**, 1237 (1995).
- ¹⁵J. J. Raftery, Jr., Ph.D. dissertation, University of Illinois at Urbana-Champaign, 2005.
- ¹⁶L. Mandel and E. Wolf, *Optical Coherence and Quantum Optics* (Cambridge University Press, New York, 1995).
- ¹⁷A. C. Lehman, J. J. Raftery, Jr., A. J. Danner, P. O. Leisher, and K. D. Choquette, *Appl. Phys. Lett.* **88**, 021102 (2006).